# Accelerometer for Mobile Robot Positioning

Hugh H. S. Liu and Grantham K. H. Pang, *Member, IEEE*

***Abstract*—An evaluation of a low-cost small-sized solid-state accelerometer is described in this paper. The sensor is intended for positioning of a mobile robot or platform. The acceleration signal output by the sensor is doubly integrated with time, which yields the traveled distance. Bias offset drift exhibited in the acceleration signal is accumulative and the accuracy of the distance measurement deteriorates with time due to the integration. This problem can be fixed by periodic recalibration by the use of external measurements on position, velocity, and attitude which can be compared with the corresponding quantities calculated by the inertial system. A Kalman filter could use the differences between those values to provide an optimum estimate of the system error. The random bias drift of the accelerometer was found experimentally to be 2.5 mg. The accelerometer was moved back and forth three times for a distance of 40 cm with an acceleration of 8 m/s$^2$. The final distance error accumulated was −1.08 cm. The bias drift rate due to temperature was 0.108 $\mu$g/s when the accelerometer was placed at room temperature. The results show that the accelerometer could be a viable solution as a short-duration distance-measuring device for a mobile robot or platform.**

***Index Terms*—Accelerometer, distance measurement.**

## I. Introduction

POSITIONING technologies can broadly be divided into two main streams: relative positioning and absolute positioning. Absolute position means that the currently calculated position does not depend on the previous positions. An example of an absolute positioning system is the Global Positioning System (GPS). The advantage of this system is that there is no accumulation of drift error. However, GPS has the signal blockage problem in the outdoor environment. Also, it cannot be used indoors and has relatively low output rate. For a relative positioning system, the dead-reckoning method is employed to find the position. The angle and distance data are used to find the current position. One of the commonly used relative positioning systems is the Inertial Navigation System (INS). Dead-reckoning positioning with gyros and accelerometers is called inertial navigation. The gyro measures the angular rate and the accelerometer senses the accelerations. Integration of angular velocity with time yields angle data. Distance data can be obtained by double integration of acceleration with time. INS is a self-contained device which requires no external electromagnetic signals. Thus, INS does not have the signal coverage problem found in GPS. Moreover, the data output rate of INS could be much faster than GPS. However, the disadvantage of INS is the bias drift problem. These errors would be accumulated and the accuracy deteriorates with time due to integration. Methods such as the Kalman filter are employed to reduce errors due to the random bias drift.

Compared to an odometer, a three-axes accelerometer can sense three-dimensional movements, while the former can only sense single-axis movements. Also, the data rate of an accelerometer can be much higher than that of an odometer. Moreover, an accelerometer is a self-contained device, while an odometer must be fixed to the shaft of some wheels, which could be inconvenient in some cases. A solid-state accelerometer also has the advantages of being small sized, having low cost, and being self-contained. Thus, this kind of accelerometer can be a viable solution as a short-duration distance-measuring device for a mobile robot or platform.

An interesting description of inertial sensors such as a solid-state gyroscope and accelerometer is given in [1]. Also, some innovative applications of the inertial sensors are proposed, such as an intelligent camera, a pen, and a shoe. Reference [2] presents a quantitative examination of the impact that an individual navigation sensor has on the performance of a navigation system. Moreover, the land vehicle application of GPS, functions, and performance of low-cost navigation sensors including a gyroscope, a compass, an odometer, and GPS are given. The sensitivity analysis of an individual sensor is also given. An evaluation of an INS consisting of a solid-state gyroscope and a solid-state accelerometer for a mobile robot can be found in [3]. An extended Kalman filter model for the thermal drift bias was built. Reference [4] described systematic and random errors in an accelerometer. Methods are proposed to reduce the effects of random errors which include proper modeling of the accelerometer and using a feedback system. A software simulation of the mathematical model of an accelerometer is also suggested in [4]. Reference [5] describes how to find the bias and scale factor errors by using inertial data and absolute position data. Reference [6] describe a low-cost GPS/INS car navigation system. GPS is used to compensate for errors such as drift rate and offset bias error for two gyroscopes and three accelerometers. The characteristics of the INS and GPS for navigation are mentioned, together with a description of hardware and software employed. Moreover, error models for the INS for the Kalman filter of the navigation system are described. In [7], Lobo *et al.* describe a prototype of an INS consisting of a piezoelectric vibrating gyro, two silicon accelerometers, two clinometers, and a magnetic compass. A robot arm was used to move the sensor in the experiments. A

Paper MSDAD-S 01–06, presented at the 1999 Industry Applications Society Annual Meeting, Phoenix, AZ, October 3–7, and approved for publication in the IEEE TRANSACTIONS ON INDUSTRY APPLICATIONS by the Industrial Automation and Control Committee of the IEEE Industry Applications Society. Manuscript submitted for review October 15, 1999 and released for publication February 27, 2001.

The authors are with the Department of Electrical and Electronic Engineering, The University of Hong Kong, Hong Kong (e-mail: hugh@graduate.hku.hk; gpang@eee.hku.hk).

Publisher Item Identifier S 0093-9994(01)03913-5.

very detailed description of individual sensors and the system architecture are given. Helsel *et al.* [8] discuss the initial results for the development of a medium-accuracy aircraft inertial navigation-grade silicon accelerometer. They aim to produce an accelerometer with a one-nautical-mile-per-hour accuracy. Their results show the feasibility of making a navigation-grade silicon micromachined accelerometer. Leonardson and Foote [9] discuss the theories and operations of a silicon micromachined accelerometer using vibrating beam accelerometer technology. They aim to produce an accelerometer which can achieve a navigation-grade performance with reduced size and lower cost. A development overview and empirical test data summary for the accelerometers are also given. In [10], Lemaire talks about the use of an accelerometer for navigation purposes. The theory, implementation, and usage of the ADXL202 accelerometer are given. Moreover, the future trend of using micromachined inertial sensors in a vehicle and personal navigation system are discussed. Barshur and Durrant-Whyte [11] give an evaluation of a low-cost solid-state inertial navigation system which consists of two gyroscopes, one triaxial accelerometer, and a tilt sensor. They also describe a field test of the INS on a land vehicle using beacon-based navigation. Kourepenis *et al.* [12] describe recent gyro and accelerometer instrument developments in their research center. Applications on micromachined inertial sensors including flight, military, and automotive are given. Allen *et al.* [13] describe a six-axes Inertial Measurement Unit (IMU) consisting of three accelerometers and three gyroscopes. Microelectromechanical systems (MEMS) technology and fabrication process are also mentioned. Results of an initial characterization test of a micromachined accelerometer is shown. A professional testing procedure for an accelerometer is described. The accelerometer evaluated is of medium performance for navigation purposes. In [14], Mostov *et al.* discuss an accelerometer-based low-cost gyro-free inertial device for automotive application. Choice of the mathematical error model of the accelerometer system, the importance of optimization of instrumentation error, and the choice of optimal sequence of elementary operations are described. The inertial system is intended for multiple automotive applications such as anti-lock brakes, adaptive power steering, and automotive navigation system. Scheding *et al.* [15] discuss the results of an experimental program for evaluating sensors and sensing technologies in an underground mining application. Barbour *et al.* [16] describe recent advances in micromechanical gyro and accelerometer design and packaging. The performance of a prototype for automotive traction control is discussed. The application of the MEMS to the automobile market is also mentioned. Kelly [17] gives some theoretical knowledge of an INS, such as theoretical mechanics, inertial sensor technologies, and stable platforms.

In this paper, the reduction of random noise of the accelerometer data using a Kalman filter is introduced in Section II. In Section III, the accelerometer and the evaluation experiment setups are described. The evaluation methods and experimental results are explained in Section IV. In Section V, discussions of the results are given. Finally, a conclusion of this paper is given in Section VI.

## II. Reduction of Random Noise Using Kalman Filter

A Kalman filter is a commonly used method for random noise reduction and data fusion for positioning applications. In this method, statistical characteristics of a measurement model is used to recursively estimate the required data. A brief introduction to the Kalman filter follows.

Kalman filtering is basically a statistical method that combines a knowledge of the statistical nature of system errors with a knowledge of system dynamics, as represented by a state-space model, to provide an estimate of the state of a system. Any number of unknowns can be included in the states. In a navigation system, we are usually concerned with position and velocity. The state estimate is obtained using a weighting function called the Kalman gain, which is optimized to produce a minimum error variance [18]. A Kalman filter can be used to blend measurements from multiple sensors and provide both an estimate of the current state of a system and a prediction of the future state of the system. The algorithm of a Kalman filter is shown in Fig. 1 [19], where $\mathbf{x_k}$ is the system state, $\mathbf{z_k}$ is the measurement, $\mathbf{w_k}$ is the plant noise with its covariance $\mathbf{Q_k}$, $\mathbf{v_k}$ is the measurement noise with its covariance $\mathbf{R_k}$, "$(-)$" indicates the *a priori* values of the variables (before the information in the measurement is used), and "(+)" indicates the *a posteriori* values of the variables (after the information in the measurement is used). $\overline{K}$ is the Kalman gain, $\Phi_k$ is the transition matrix at time $\mathrm{t_k}$, $P_k$ is the error covariance matrix, and $H_k$ is the measurement matrix, whereas

$$\phi_k = \begin{bmatrix} 1 & \Delta t & \Delta t^2/2 \\ 0 & 1 & \Delta t \\ 0 & 0 & 1 \end{bmatrix}$$

$$Q_k = \begin{bmatrix} \frac{W}{20}\Delta t^5 & \frac{W}{8}\Delta t^4 & \frac{W}{6}\Delta t^3 \\ \frac{W}{8}\Delta t^4 & \frac{W}{3}\Delta t^3 & \frac{W}{2}\Delta t^2 \\ \frac{W}{6}\Delta t^3 & \frac{W}{2}\Delta t^2 & W\Delta t \end{bmatrix}.$$

The accelerometer bias is modeled as a random walk process as shown in Fig. 2. This bias is modeled as integrated white noise with power spectral density (PSD) being $W$. The complete process is modeled by three integrators in cascade, as shown in Fig. 2 [20]. From this model, the exact expressions for $\phi_k$ and $Q_k$ can be worked out in the form as shown above. The PSD of the input white noise $W$ is $1(\mathrm{m/s^2})^2/(\mathrm{rad/s})$, and the sampling time $\Delta t$ equals 1/206.6 s. The value of $W$ was obtained after some experiments to provide better results.

## III. Accelerometer Evaluation Experimental Setups

### A. Accelerometer

The accelerometer (interface circuit shown in Fig. 3) that has been evaluated is the ADXL202 produced by Analog Devices, Inc. It is a low-cost low-power two-axes micromachined accelerometer with a measurement range of $\pm 2$ g (19.6 $\mathrm{m/s^2}$). It

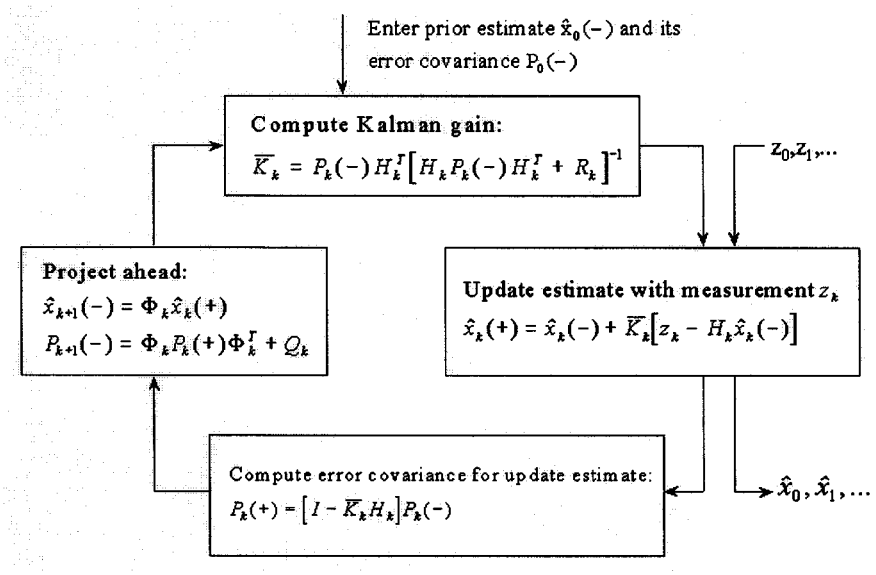


Fig. 1. Kalman filter algorithm.

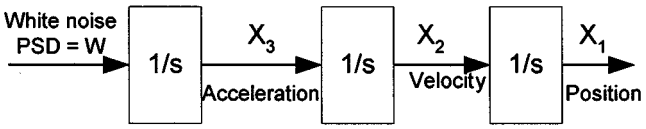


Fig. 2. Process model of the accelerometer data for the Kalman filter.

can measure both dynamic acceleration and static acceleration. The outputs are digital signals with duty cycles proportional to the acceleration in each of the two axes [21]. The output can be measured directly with a micro-controller unit (MCU) timer system. This accelerometer is selected for evaluation as a distance-measuring sensor due to its small size, low cost, and acceptable performance. The sampling rate of the accelerometer depends on the dynamic of the robot. If a high-speed robot is used, the accelerometer should be set to a higher bandwidth, which requires a faster sampling rate. The bandwidth of our evaluated accelerometer is from 0.01 Hz to 5 kHz. In our case, a bandwidth of 50 Hz and a sampling rate of 200 Hz were used. However, wider bandwidth would cause higher white noise in the signal.

### *B. Microcontroller and Data Acquisition Board*

The microcontroller used in the data acquisition board is a Motorola 68HC11F1. It has 512 bytes of electrically erasable and programmable read-only memory (EEPROM), 1024 bytes of RAM, an enhanced 16-bit timer system, three input capture (IC) channels, and an enhanced nonreturn to zero (NRZ) serial communications interface (SCI) [22]. The data acquisition circuit board is shown in Fig. 4.

The data output by the accelerometer is a 200-Hz square wave whose duty cycle depends on the acceleration. The IC1 pin of the MCU was used to detect the signal from the accelerometer. The MCU would transmit the data to the PC via the SCI. A Visual Basic program was used at the PC to receive and save the data to the hard disk. A C program was written to process

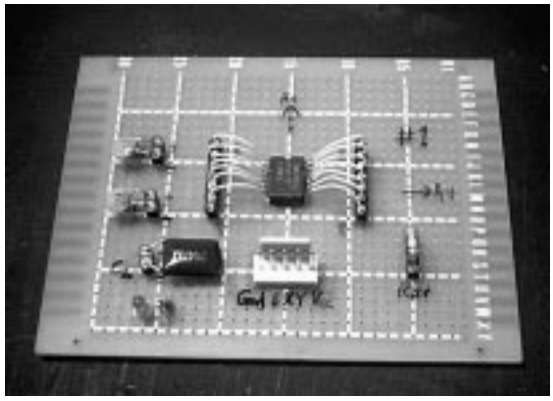

Fig. 3. Accelerometer interface board.

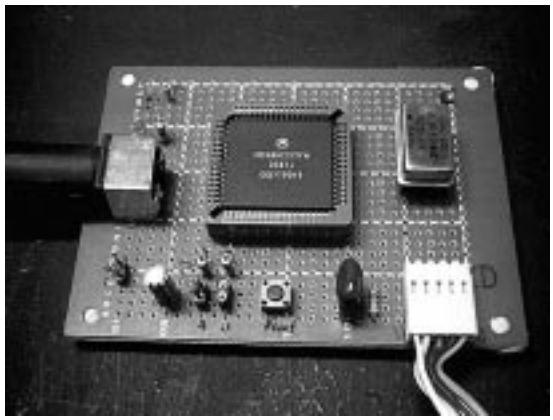

Fig. 4. Data acquisition board with the microcontroller.

large amounts of accelerometer data. The recorded data is downsampled by averaging the acceleration data within each downsampling period. The downsampled data was then stored in a file which could be plotted using MATLAB. For the results obtained, the data was averaged every 25 s to give downsampled data.

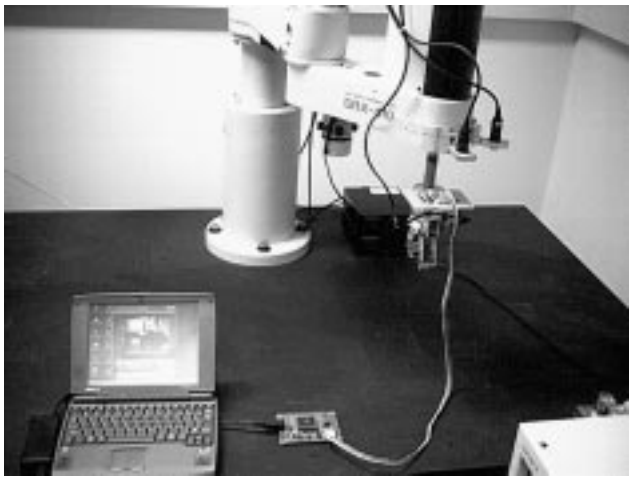

Fig. 5. Accelerometer evaluation experiment hardware setup.

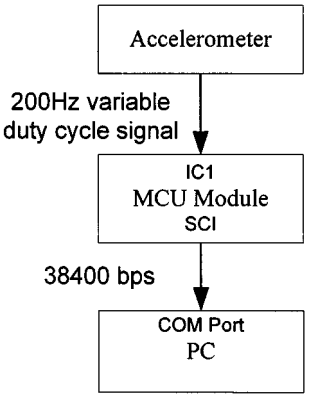


Fig. 6. Accelerometer data acquisition block diagram.

### C. Sony Robot Arm

The robot arm used to move the accelerometer is a Sony SRX-410 High Speed Assembly Robot. It was designed for high assembling speed and high-performance industrial applications. The system consists of a robot arm, a controller, a panel, and a PC for programming the robot arm. Fig. 5 shows a photograph of the accelerometer evaluation hardware setup. The block diagram of the experimental setup is shown in Fig. 6.

## IV. Evaluation Methods and Experimental Results

### A. Thermal Bias Drift

Fourteen hours of stationary accelerometer data was taken in order to study the effect of temperature on the bias drift. The recorded data occupied 81.3 Mbytes of hard disk space. The data were processed to give the acceleration readings which were then downsampled for plotting using MATLAB.

The duty cycle of the accelerometer output is proportional to the acceleration. The microcontroller was used to measure the duty cycle using the timer system. The timer counts were converted to ASCII and then sent to the PC for recording. The data were processed according to Fig. 7.

Figs. 8 and 9 show the 14 h of stationary accelerometer data without and with Kalman filter processing, respectively. The thermal bias drift rate of the accelerometer placed at room temperature was found by this experiment to be 0.108 $\mu$g/s.

### B. Experiments Carried Out Using Sony Robot Arm

Experiments for the accelerometer evaluation were carried out using the Sony Robot Arm. Twenty-three sets of experiments with different velocity and acceleration combinations were conducted. The velocities range from 0 to 1 m/s and the accelerations range from 0 to 10 m/s$^2$. Three different sets of results with low, moderately high, and high acceleration are presented in the following sections.

*1) Low Acceleration ($a$ = 3 m/s$^2$):* Figs. 10–13 show the results of the experiment with acceleration at 3 m/s$^2$, which is quite low, and with velocity at 0.3 m/s. The accelerometer was moved from left to right and vice versa for a distance of 40 cm. Such motions were repeated three times. Figs. 10 and 11 show the acceleration data without and with Kalman filtering. Due to the random bias drift problem, the acceleration data were divided into regions for different bias reductions. The biases in the first seven regions were manually tuned to optimize the accuracy. The last six regions were not calibrated for comparison purposes. These calibrations also helped to estimate the random bias drift of the accelerometer. The values of the manually tuned biases are plotted in Fig. 14. Fig. 12 shows the velocity which was calculated by integrating the acceleration data with time. Only the first two velocity cycles are calibrated with manually tuned acceleration biases. Fig. 13 shows the distance which was calculated by integrating the velocity data with time. Only the first two distance cycles are calibrated with manually tuned acceleration biases. This graph shows the affect of the random bias drift on the distance data after double integration of the accelerometer data.

*2) Moderately High Acceleration ($a$ = 8 m/s$^2$):* Figs. 15–18 show the results of the experiment with acceleration at 8 m/s$^2$ which is quite high and with velocity at 0.8 m/s. Again, the accelerometer was moved from left to right and vice versa for a distance of 40 cm. Such motions were repeated three times. The acceleration was calibrated with a constant bias to reduce the zero offsets.

Fig. 15 shows the acceleration data without Kalman filter processing. This has resulted in a signal disturbed with random noises. A clearer shape of the signal obtained by using a Kalman filter is shown in Fig. 16. The integrated velocity is shown in Fig. 17, and the integrated distance is shown in Fig. 18. The final distance was found to be $-1.08$ cm, while the actual final distance should be zero.

*3) High Acceleration ($a$ = 10 m/s$^2$):* Figs. 19–22 show the results of the experiment with acceleration equal to 10 m/s$^2$, which is relatively high, and velocity equals 1 m/s. The accelerometer was moved from left to right and vice versa for a distance of 40 cm. Such motions were repeated eight times. The acceleration was calibrated with a constant bias to reduce the zero offsets.

Figs. 19 and 20 show the acceleration without and with Kalman filter processing, respectively. The velocity and the distance are shown in Figs. 21 and 22 respectively. The final distance was found to be $+1.55$ cm.

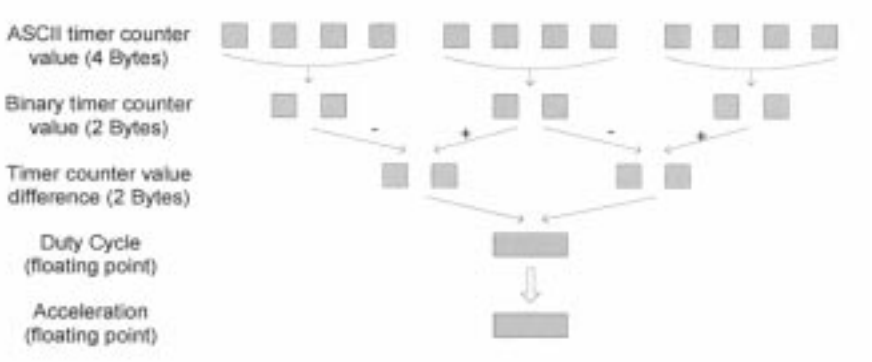


Fig. 7. Data processing diagram for the acceleration data.

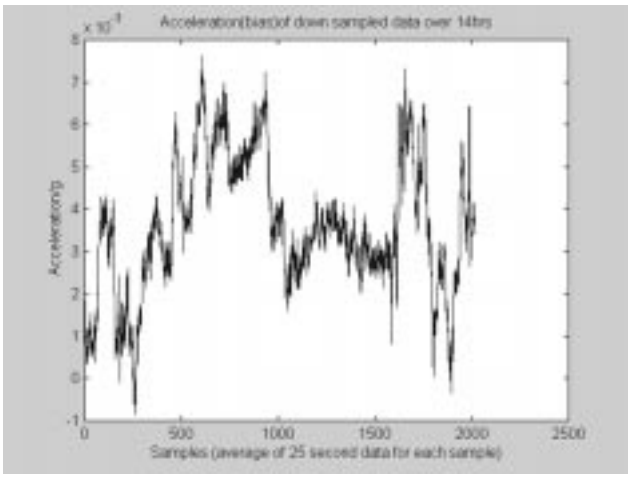


Fig. 8. Acceleration data in 14 h without Kalman filter processing.

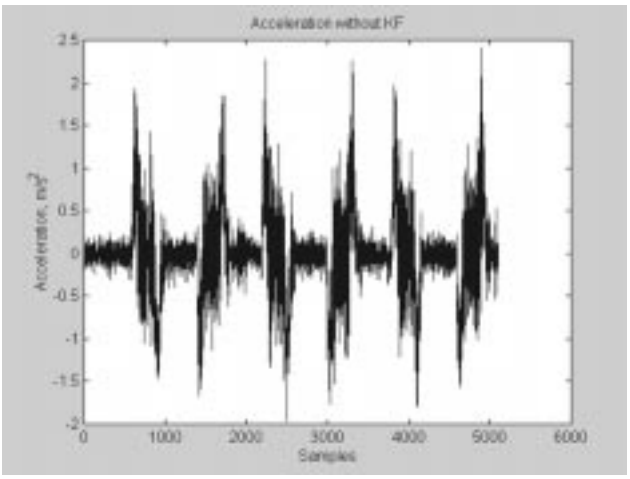


Fig. 10. Acceleration at 3 m/s$^2$ without Kalman filtering.

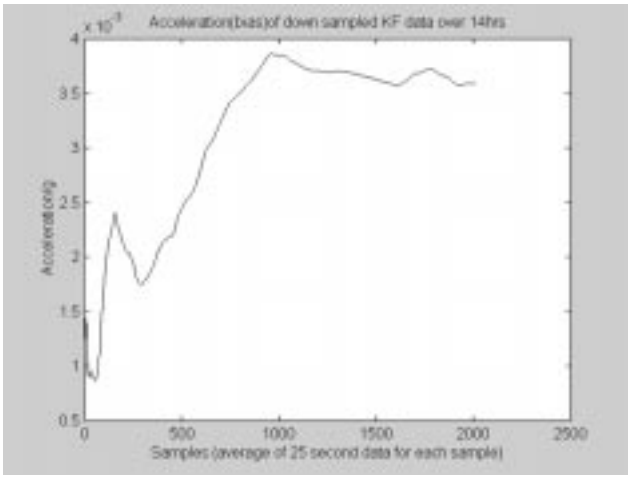


Fig. 9. Acceleration data in 14 h with Kalman filter processing.

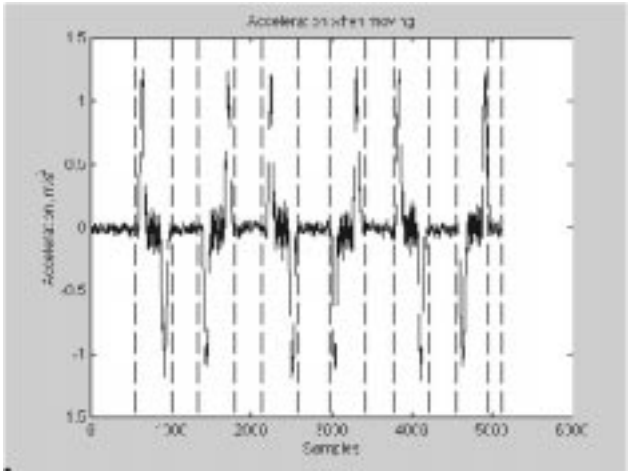


Fig. 11. Acceleration after Kalman filtering with bias calibration.

## V. Discussions

### A. Behavior of the 14-h Stationary Accelerometer Data

From the result shown in Fig. 9, it is observed that the bias or zero offset of the accelerometer generally increased after powering up. After about 7 h, the bias settled down to fairly stable values. The results are due to the thermal bias drift of the accelerometer. The internal temperature of the sensor increases when it is warming up. The thermal bias drift rate when the accelerometer is placed at room temperature is found in this evaluation to be 0.108 $\mu$g/s. If these bias drifts due to the temperature are not compensated, the results would be affected after operating for a long duration. Compensation methods can be done by using a low-cost temperature-sensing IC and crystal oven [23].

### B. Experiments Carried Out Using Sony Robot Arm

*1) Random Bias Drift:* The effects of the random bias drift on the velocity and position error on the accelerometer are de-

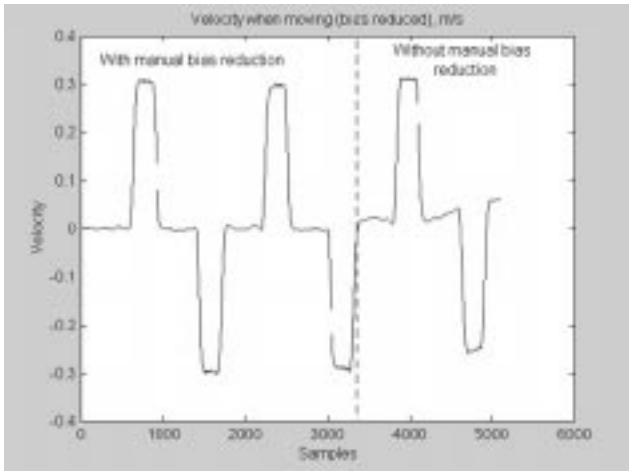


Fig. 12. Velocity with and without manually tuned acceleration biases reduction (only first two velocity cycles are calibrated).

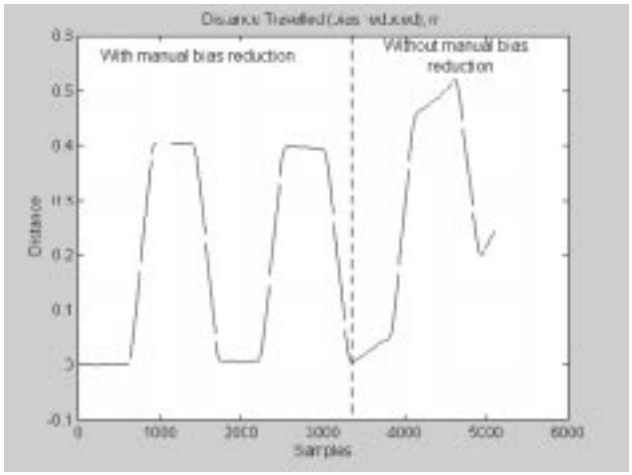


Fig. 13. Distance traveled with and without manually tuned acceleration biases reduction (only the first two distance cycles are calibrated).

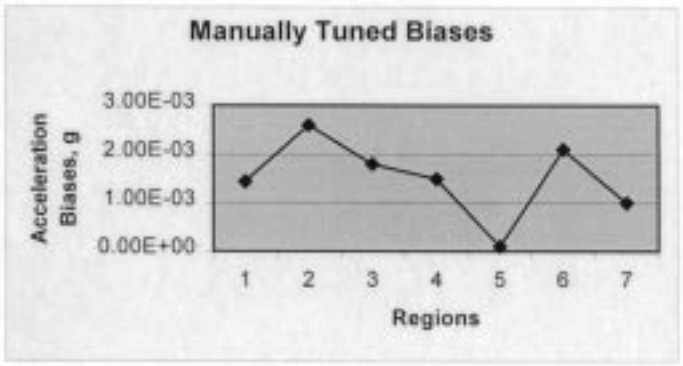


Fig. 14. Manually tuned biases for the first seven regions of the acceleration data.

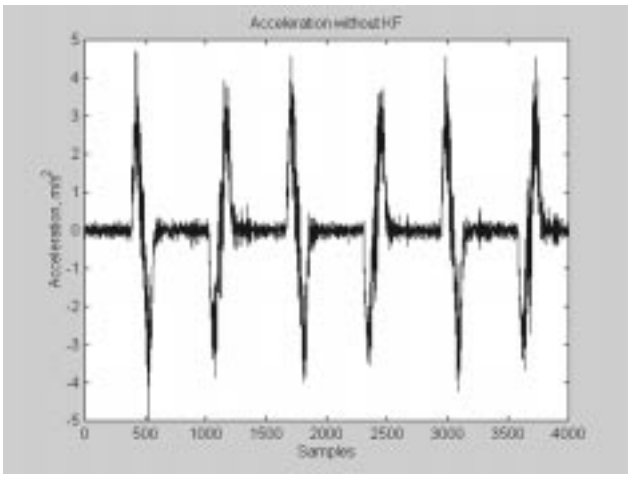


Fig. 15. Acceleration results for acceleration of 8 m/s$^2$ and velocity of 0.8 m/s without Kalman filter processing.

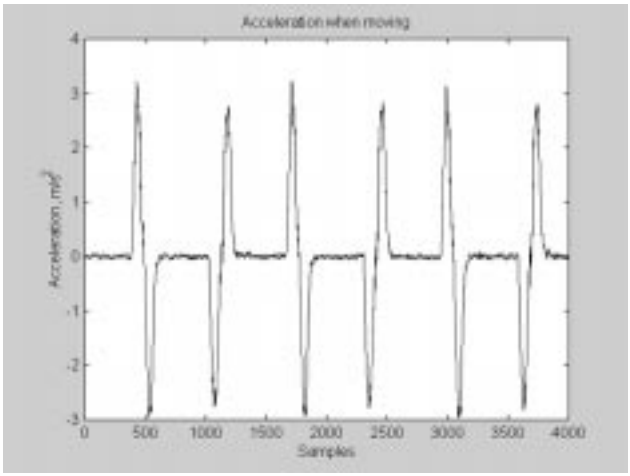


Fig. 16. Acceleration results for acceleration of 8 ms$^{-2}$ and velocity of 0.8 ms$^{-1}$ with Kalman filter processing.

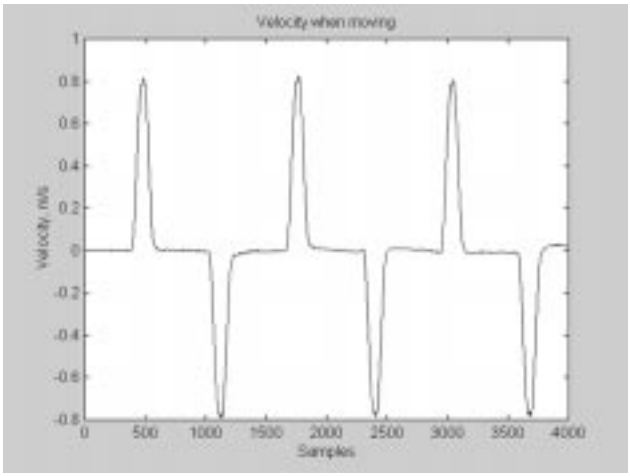


Fig. 17. Integrated velocity results for acceleration of 8 ms$^{-2}$ and velocity of 0.8 ms$^{-1}$.

scribed in this section. From the graph of manually tuned biases (Fig. 14), the range of the biases deviations is about 2–3 mg, which is fairly large. A better navigational-grade accelerometer has about 0.1-mg random bias drift. The velocity error and the position error built up could be calculated by the following equations [24]:

$$\text{velocity error} = 0.589 \text{ m/s per mg per min}$$

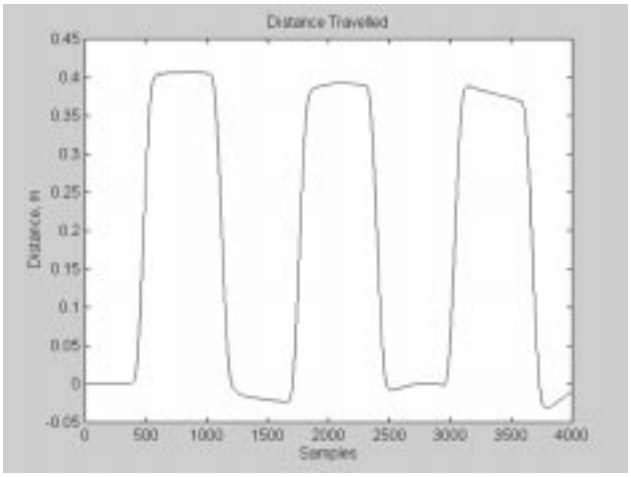


Fig. 18. Integrated position results for acceleration of 8 $ms^{-2}$ and velocity of 0.8 $ms^{-1}$.

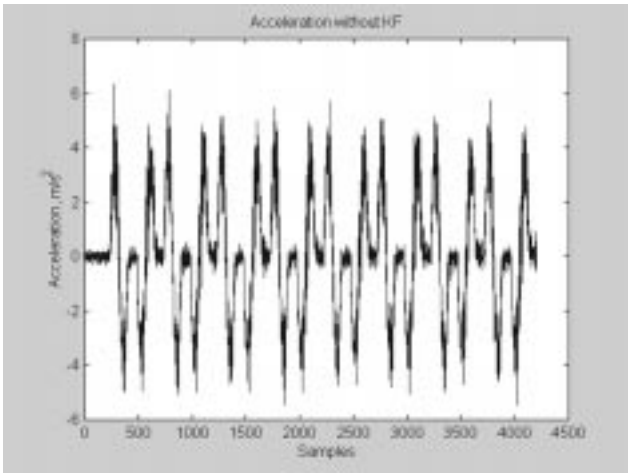


Fig. 19. Acceleration results for acceleration of 10 $ms^{-2}$ and velocity of 1 $ms^{-1}$ without Kalman filter processing.

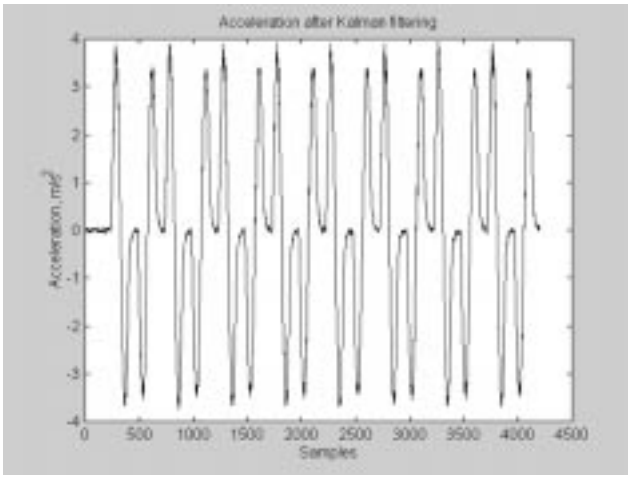


Fig. 20. Acceleration results for acceleration of 10 $ms^{-2}$ and velocity of 1 $ms^{-1}$ with Kalman filter processing.

$$\text{position error} = 17.66 \text{ m per mg per min}^2.$$

If the bias drift is small (for example, 0.1 mg), the positioning error is 1.76 m per minute, which can be considered small. For a bias error of 2 mg, the velocity error built up in 1 min is 1.178 m/s. Moreover, the position error built up in 1 min for a bias error of 2 mg is 35.32 m. Thus, if the random bias could be modeled properly, the accuracy in distance measurement can be greatly improved. The system can also be recalibrated periodically by the use of external measurements on position, velocity, and attitude. The external measurements can be compared with the corresponding quantities calculated by the inertial system, and the Kalman filter would use the differences between those values to provide an optimum estimate of the system error.

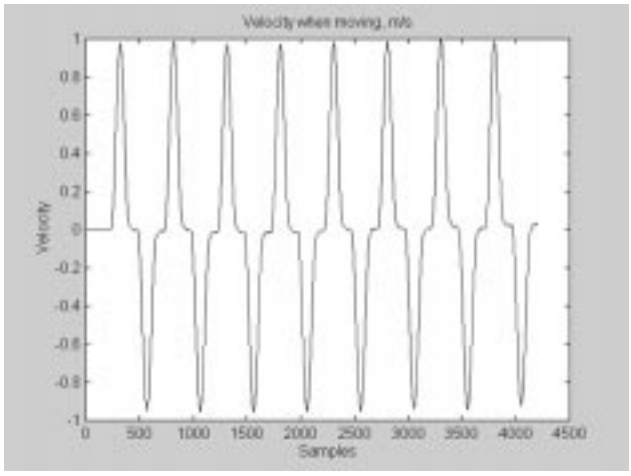


Fig. 21. Velocity results for acceleration of 10 $ms^{-2}$ and velocity of 1 $ms^{-1}$.

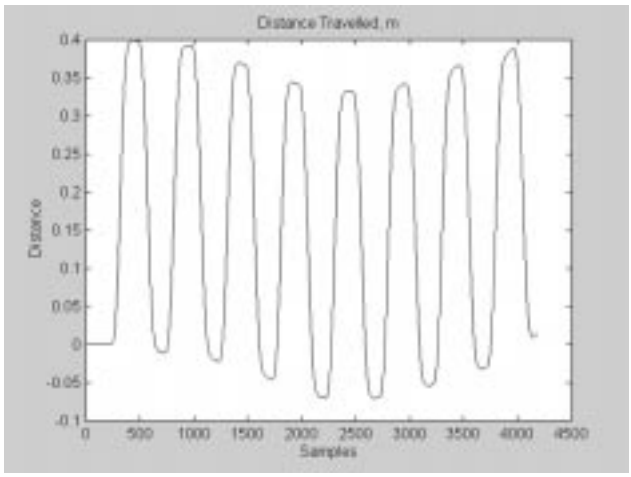


Fig. 22. Distance results for acceleration of 10 $ms^{-2}$ and velocity of 1 $ms^{-1}$.

*2) Relation Between Magnitude of Acceleration and Accuracy in Distance Measurement:* From the distance graphs of Figs. 18 and 22, distortions are observed which were due to the random biases of the accelerometer. The bending shape of the curve in Fig. 22 is due to the doubly integrated error of the acceleration bias drift. The polarity of the drift error can be positive or negative. In the first 2200 samples, there was a negative bias error in the acceleration data. This caused the position plot to be shifted downward. However, for the next 2000 samples, the position plot was shifted upward, which is due to a positive acceleration drift error. The random bias drift error is one of the major sources of the positioning error. When the acceleration is higher, the errors caused by the random bias are less significant.

The integrated final distance was found to be $-1.08$ cm and $+1.55$ cm when the accelerations were 8 m/s$^2$ and 10 m/s$^2$, while the actual final distances should both be zero. Thus, the results are quite close to the ideal ones. These good results were due to the relatively large acceleration imposed on the accelerometer. As the accelerometer can measure up to 2 g, which is 19.6133 m/s$^2$ of acceleration, the applied accelerations which are 8 m/s$^2$ and 10 m/s$^2$ are relatively large. When compared with Fig. 13, the distortions in distance measurement for higher accelerations are less. This means that, when the acceleration is higher, the errors caused by the random biases are less significant.

## VI. Conclusions

The experimental results have provided a useful evaluation of a low-cost solid-state accelerometer. The performance of the accelerometer is shown to be acceptable as a short-duration distance-measuring device for mobile platform or robot. With 2 mg of random bias drift, the low-cost accelerometer could be considered as acceptable for high dynamic robot operation with suitable periodical recalibration from external measurements on position, velocity, and attitude. Such an accelerometer could be a self-contained sensor to give a low-cost and small-sized distance-measuring device for a mobile robot, platform, or vehicle. It can be combined with a gyroscope and odometer to form a dead-reckoning positioning system for a mobile robot or platform. Further research would focus on the proper modeling of the accelerometer in order to reduce the effect of random bias drift.

## References


[1] C. Verplaetse, "Inertial proprioceptive devices: Self-motion sensing toys and tools," *IBM Syst. J.*, vol. 35, no. 3 and 4, pp. 647–649, 1996.

[2] E. Abbott and D. Powell, "Land-vehicle navigation using GPS," *Proc. IEEE*, vol. 87, pp. 145–162, Jan. 1999.

[3] B. Barshan and H. F. Durrant-Whyte, "An inertial navigation system for a mobile robot," in *Proc. Int. Conf. Intelligent Robots and Systems*, Yokohama, Japan, 1993, pp. 2243–2248.

[4] K. Mostov, Inertial sensor documentation, Web Page of PATH, Univ. California, Berkeley. [Online]. Available: http://www.path.berkeley.edu/~webed/sensor/papers.html

[5] K. Mostov, Method for correction of systematic inertial sensor error, Web Page of PATH, Univ. California, Berkeley. [Online]. Available: http://www.path.berkeley.edu/~webed/sensor/papers.html

[6] J.-S. Gil, Y.-D. Cho, and S.-H. Kim, "Design of a low-cost inertial navigation system with GPS for car navigation system," in *Proc. 5th World Congr. ITS*, 1998, Paper 4057, CD-ROM.

[7] J. Lobo, P. Lucas, J. Dias, and A. T. de Almeida, "Inertial navigation system for mobile land vehicles," in *Proc. IEEE Int. Symp. Industrial Electronics*, vol. 2, 1995, pp. 843–848.

[8] M. Helsel, G. Gassner, M. Robinson, and J. Woodruff, "A navigation grade micro-machined silicon accelerometer," in *Proc. IEEE Position Location and Navigation Symp.*, 1994, pp. 51–58.

[9] R. Leonardson and S. Foote, "SiMMA accelerometer for inertial guidance and navigation," in *Proc. IEEE Position Location and Navigation Symp.*, 1998, pp. 152–160.

[10] C. Lemaire, "Surface micromachined sensors for vehicle and personal navigation system," in *Proc. IEEE ITSC'97*, 1997, pp. 1068–1072.

[11] B. Barshan and H. F. Durrant-Whyte, "Inertial navigation systems for mobile robots," *IEEE Trans. Robot. Automat.*, vol. 11, pp. 328–342, June 1995.

[12] A. Kourepenis, J. Borenstein, J. Connelly, R. Elliott, P. Ward, and M. Weinberg, "Performance of MEMS inertial sensors," in *Proc. IEEE Position Location and Navigation Symp.*, 1998, pp. 1–8.

[13] J. J. Allen, R. D. Kinney, J. Sarsfield, M. R. Daily, J. R. Ellis, J. H. Smith, S. Montague, R. T. Howe, B. E. Boser, R. Horowitz, A. P. Pisano, M. A. Lemkin, W. A. Clark, and T. Juneau, "Integrated micro-electromechanical sensor development for inertial applications," in *Proc. IEEE Position Location and Navigation Symp.*, 1998, pp. 9–16.

[14] K. S. Mostov, A. A. Soloviev, and T.-K. J. Koo, "Accelerometer based gyro-free multi-sensor generic inertial device for automotive applications," in *Proc. IEEE Intelligent Transportation System Conf.*, 1997, pp. 1047–1052.

[15] S. Scheding, E. M. Nebot, M. Stevens, H. Durrant-Whyte, J. Roberts, P. Corke, J. Cunningham, and B. Cook, "Experiments in autonomous underground guidance," in *Proc. IEEE Int. Conf. Robotics and Automation*, 1997, pp. 1898–1903.

[16] N. Barbour, E. Brown, J. Connelly, J. Dowdle, G. Brand, J. Nelson, and J. O'Bannon, "Micromachined inertial sensors for vehicle," in *Proc. IEEE Conf. Intelligent Transportation Systems*, 1997, pp. 1058–1063.

[17] A. Kelly, "Modern inertial and satellite navigation system," Carnegie-Mellon Univ., Pittsburgh, PA, 1994.

[18] E. D. Kaplan, *Understanding GPS: Principle and Applications*, 1st ed. Boston, MA: Artech House, 1996, p. 39.

[19] R. G. Brown and P. Y. C. Hwang, *Introduction to Random Signals and Applied Kalman Filtering*, 3rd ed. New York: Wiley, 1997, p. 219.

[20] R. G. Brown and P. Y. C. Hwang, *Introduction to Random Signals and Applied Kalman Filtering*, 3rd ed. New York: Wiley, 1997, p. 232.

[21] Analog Devices, Inc., Santa Clara, CA, ADXL202 data sheet, 1998.

[22] Motorola, Inc., Schaumburg, IL, 68HC11F1 technical data, 1995.

[23] C. Kitchin, "Understanding accelerometer scale factor and offset adjustments," Analog Devices, Inc., Santa Clara, CA, 1995.

[24] A. Lawrence, *Modern Inertial Technology*. Berlin, Germany: Spring-Verlag, 1993, p. 28.


**Hugh H. S. Liu** received the B.Eng. and M.Phil. degrees from the Department of Electrical and Electronic Engineering, The University of Hong Kong, Hong Kong, in 1997 and 2000, respectively.

Since graduation, he has been a Design Engineer for a visual inspection system project in the Industrial Automation Laboratory, The University of Hong Kong. His research interests include vehicle positioning sensors and systems, intelligent transportation systems, vision systems and circuits, and image processing.

**Grantham K. H. Pang** (S'84–M'86) received the Ph.D. degree from the University of Cambridge, Cambridge, U.K., in 1986, for research in multivariable control system design and expert systems.

He was with the Department of Electrical and Computer Engineering, University of Waterloo, Waterloo, ON, Canada, from 1986 to 1996. He joined the Department of Electrical and Electronic Engineering, The University of Hong Kong, Hong Kong, in 1996. Since 1988, he has authored more than 120 published technical papers and has authored or coauthored three books. His research interests include expert systems for control system design, intelligent control, intelligent transportation systems, neural networks, control theory, and computer-aided design. In 1994, he was a Senior Visiting Researcher at the Hitachi Research Laboratory, Japan. He has acted as a Consultant to many companies, including Mitsubishi Electric Corporation, Japan, and Northern Telecom and Imperial Oil Ltd., Canada. He is an Editor of the *International Journal of Intelligent Control and Systems* and the *Journal of Control and Computers* (published by the International Association of Science and Technology for Development).

Dr. Pang was the Organizing Chair of the 1996 IEEE Symposium on Computer-Aided Control System Design. He was appointed by the President of the IEEE Control Systems Society as the Chair of the Technical Committee on Computer-Aided Control System Design (1993–1995). In 1989, he was awarded the ICI Prize for authorship of the best paper on the application of the theory of control published in the *Transactions of the Institute of Measurement and Control*. He is a Chartered Electrical Engineer in the U.K. and a member of the Institution of Electrical Engineers, U.K., and Hong Kong Institution of Engineers.